Supporting Information

Single Crystal to Single Crystal Polymerization of a Self-Assembled Diacetylene Macrocycle Affords Columnar Polydiacetylenes

Weiwei L. Xu,[a] Mark D. Smith,[a] Jeanette A. Krause,[c] Andrew B. Greytak,[a] Shuguo Ma,[b] Cory M. Read[a] and Linda S. Shimizu*[a]

[a] Department of Chemistry and Biochemistry and [b] College of Engineering and Computing, University of South Carolina, Columbia, South Carolina, 29203, United States

[c] The Richard C. Elder X-ray Crystallographic Facility, Department of Chemistry, University of Cincinnati, Cincinnati, Ohio 45211, United States

shimizls@mailbox.sc.edu

NMR characterizations: ^{1}H, ^{13}C-NMR of diamide intermediate and macrocycle **1** were recorded on Varian Mercury/VX 300 and 400 NMR spectrometer.

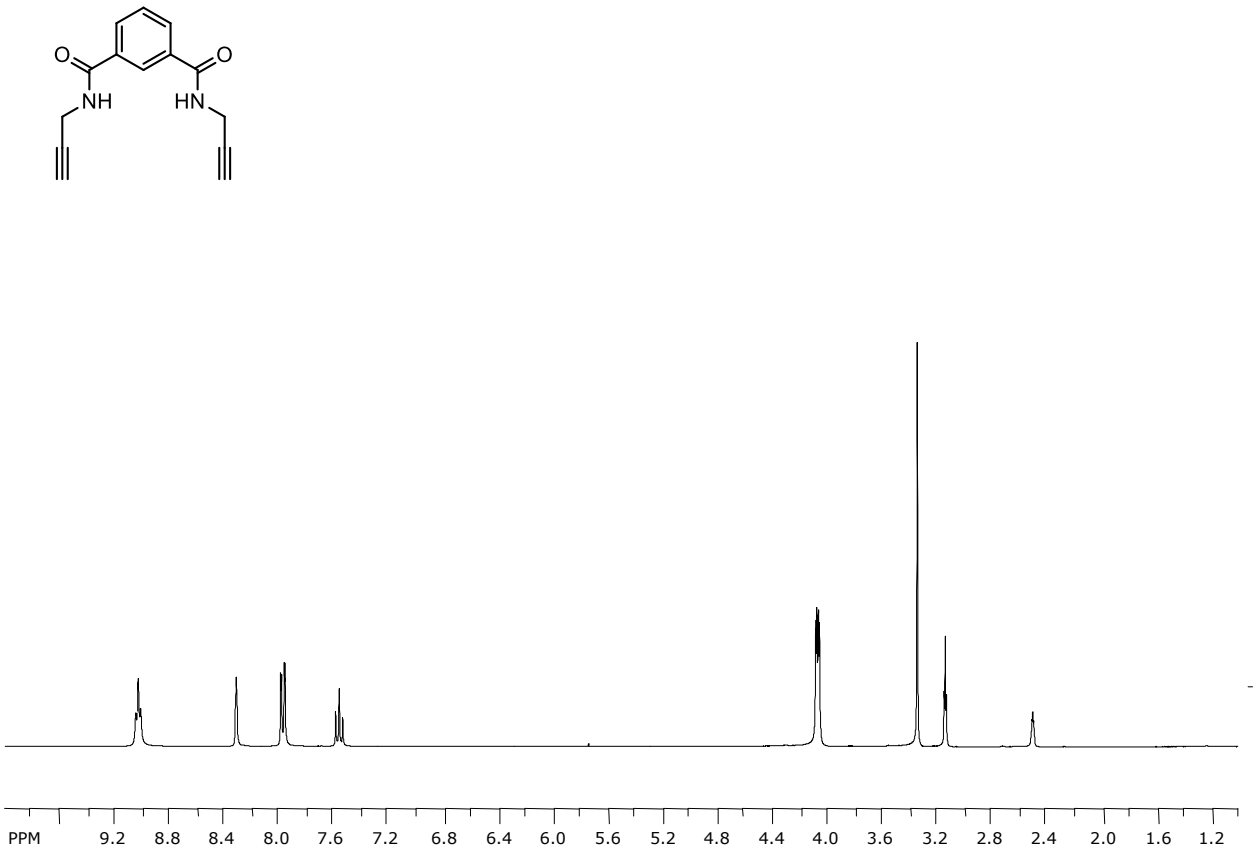

Figure S1. ^{1}H NMR of the diamide intermediate in DMSO-d_6.

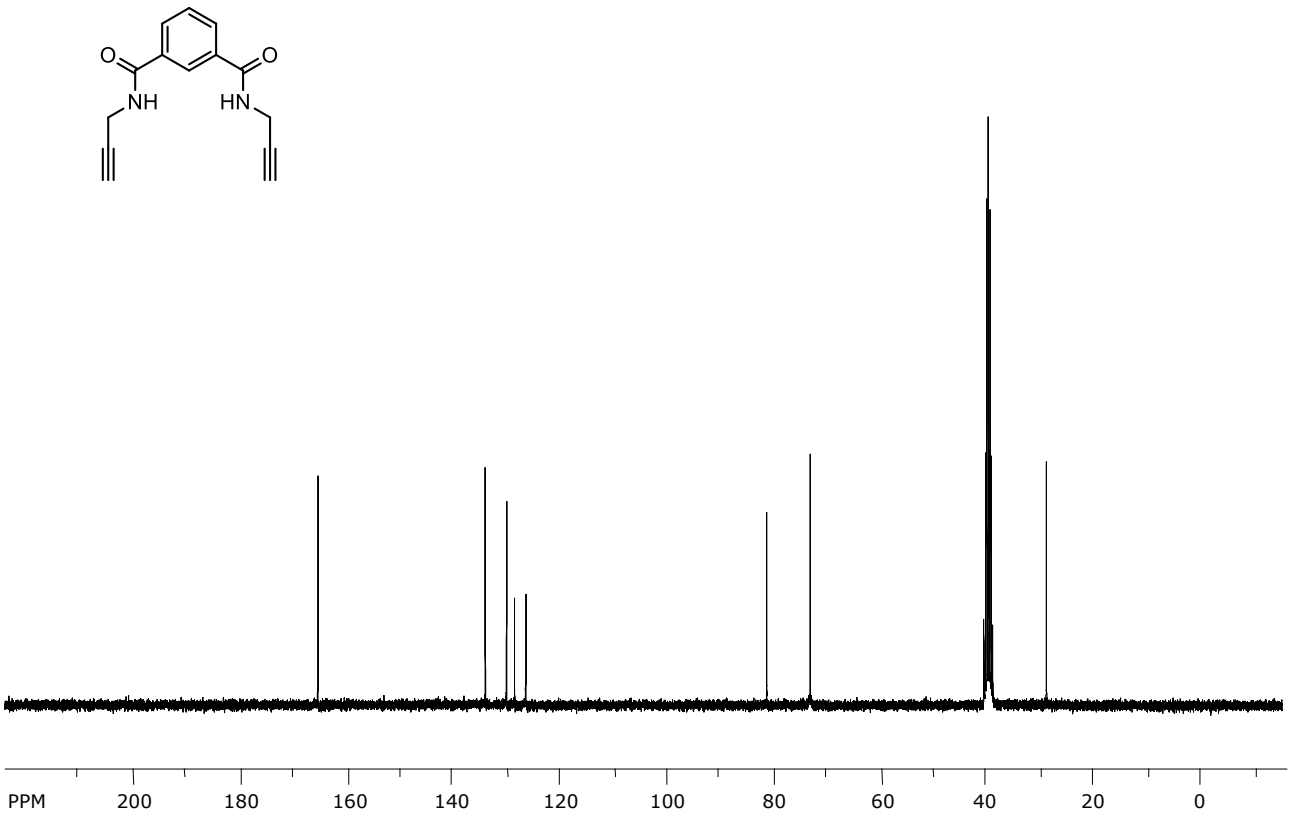

Figure S2. ^{13}C NMR of the diamide intermediate in DMSO-d_6.

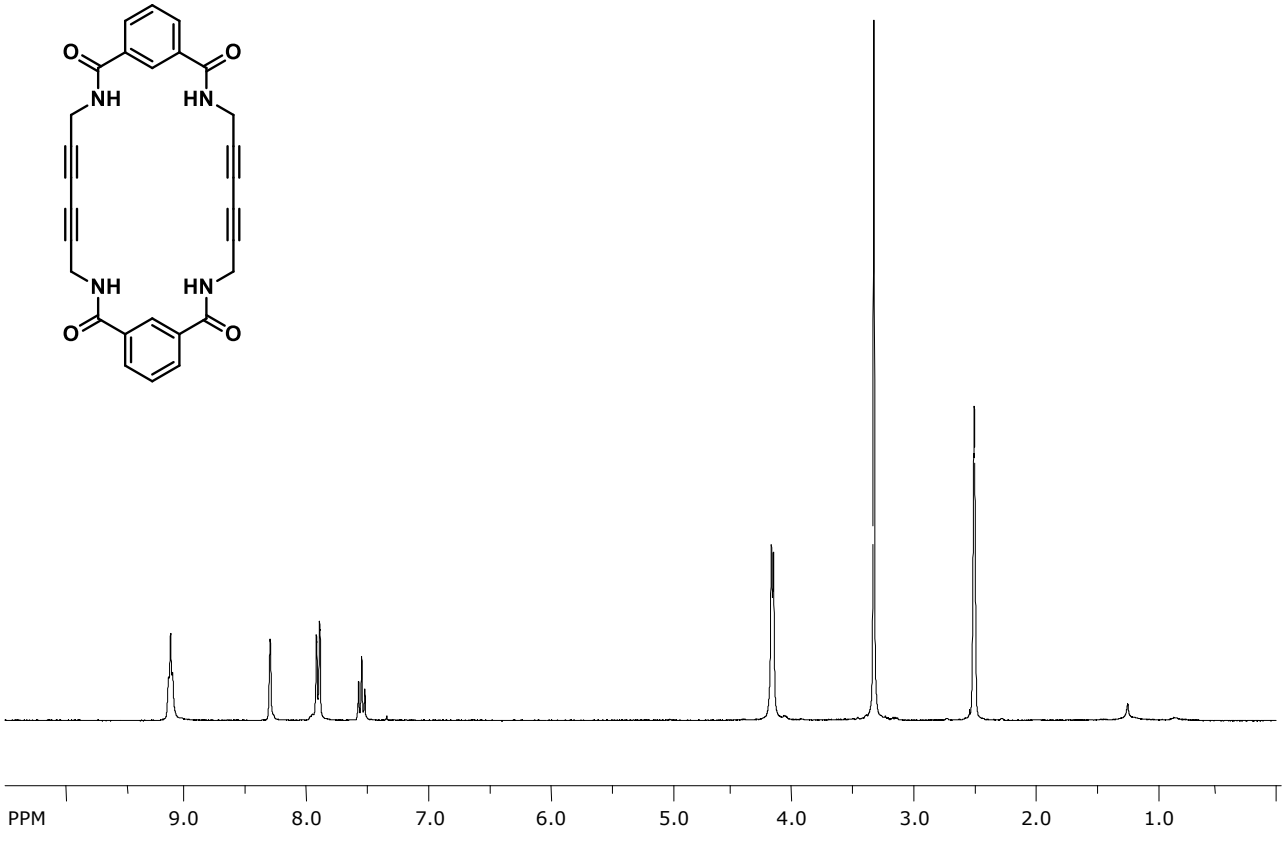

Figure S3. ^{1}H NMR of the macrocycle **1** in DMSO-d_6.

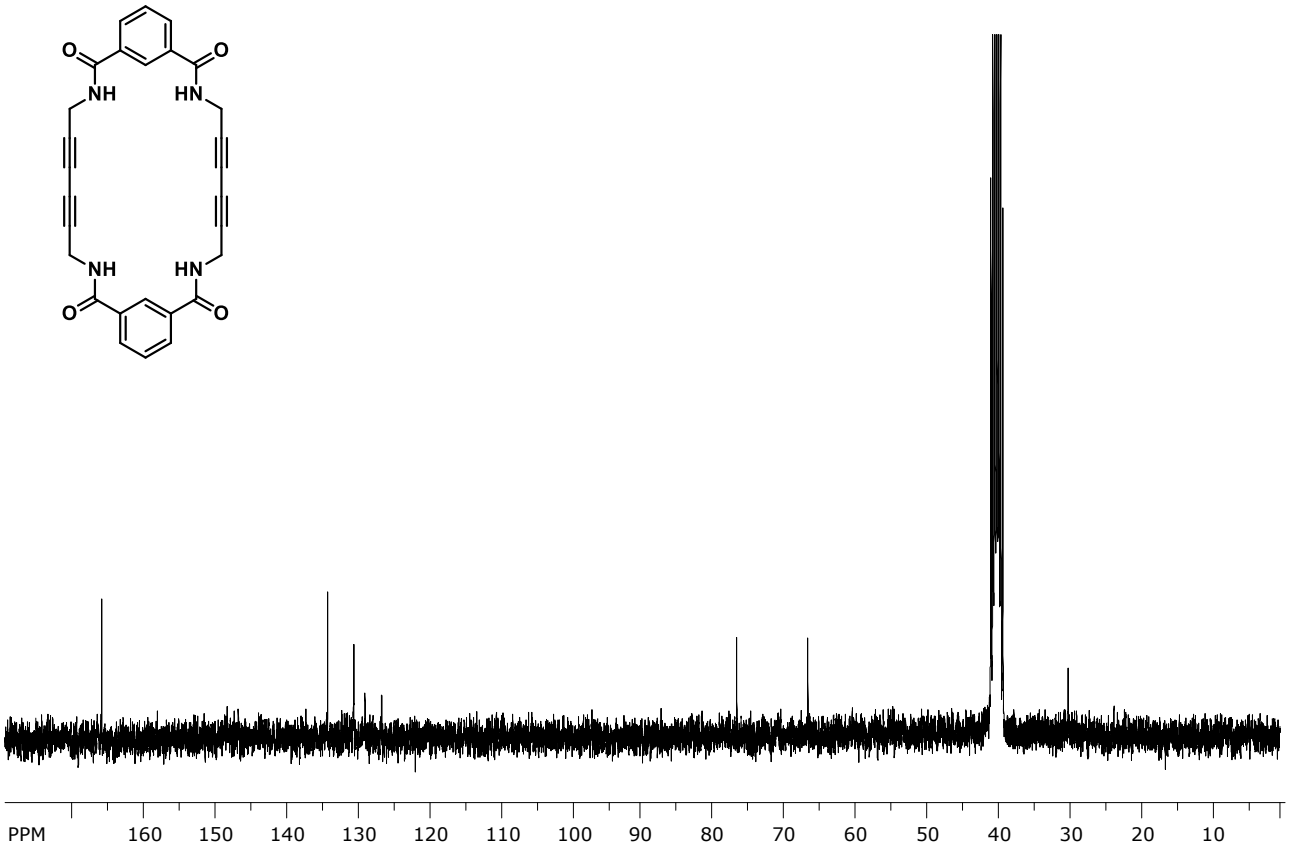

Figure S4. ^{13}C NMR of the macrocycle **1** in DMSO-d_6.

$C_{28}H_{20}N_4O_4 \cdot 2H_2O$: Crystals of assembled macrocycle **1** were obtained through slow evaporation of macrocycle **1** in 45:55:5 MeOH/CH_2Cl_2/H_2O (conc. 2 mg/mL). The **1**•2H_2O crystals were sensitive to light. The crystals turned from colorless to reddish after exposure to light over several days, which indicated a small percentage of polymerization of the crystal, but this small amount of polymer was at a level that could not be detected by single X-ray analysis. The presence of some oligo- or polydiacetylene was further suggested by the Raman spectra, which shown the two characteristic resonance bands (located at ~1506 and ~2107 cm^{-1}) of polydiacetylene.

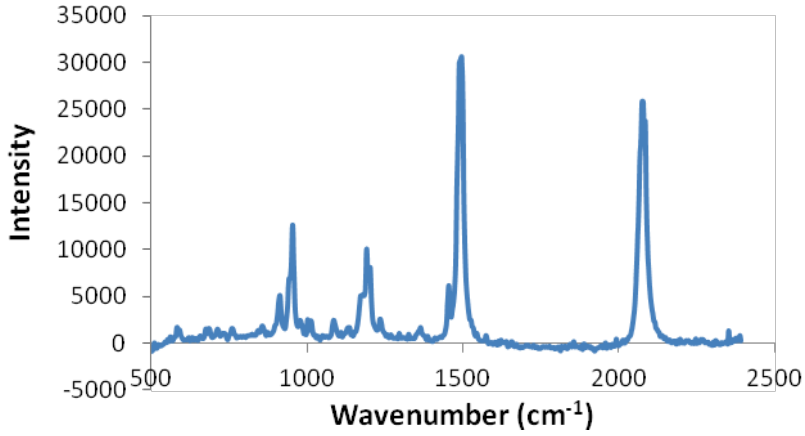

Figure S5. Raman spectrum of **1**•2H_2O crystals.

After heating at 190 °C for 12 h under N_2 gas, the **1**•2H_2O bulk crystals turned dark purple/brown in color, and the product was not soluble in most common solvents. Therefore solid-state ^{1}H-^{13}C COSY (HETCOR) was used to further analyze the structure. We observed broad peaks for the heated product (Figure S6), which is typical of polymers. In the ^{13}C NMR of the heated sample, two significant chemical shifts were seen at 100-110 ppm, and no correlated chemical shifts were found in the corresponding ^{1}H NMR, thus these two peaks should be assigned to the newly formed C=C bonds. No non-polymerized acetylene peaks were observed in the ^{13}C spectrum, which indicated a high conversion of polymerization reaction. The ^{13}C single of –CH_2 was found at 44 ppm,[1] compared with the chemical shift of methylene group in macrocycle **1** (29-32 ppm),[2] the peak was shifted downfield by 14 ppm, which should be due to the transformation from the methylene to conjugated allylic system during the polymerization process. Thus, the solid-state ^{1}H-^{13}C COSY of thermally-treated bulk **1**•2H_2O crystals gave strong evidence for the formation of the PDA.

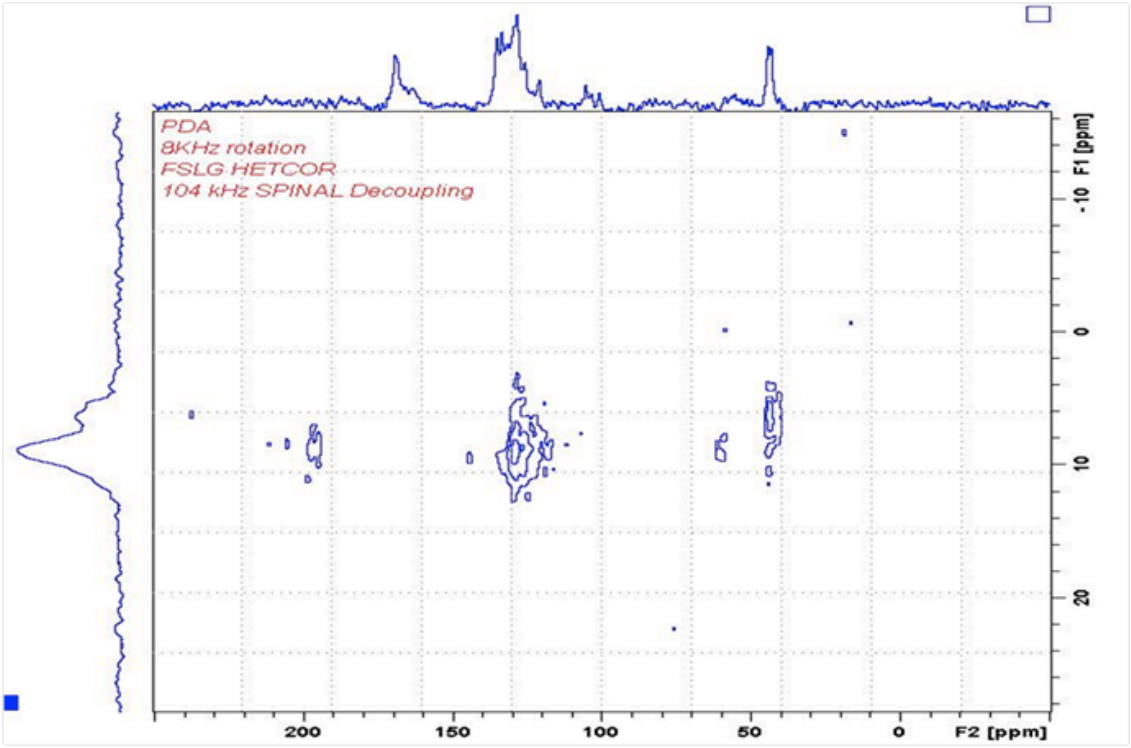

Figure S6. Solid-state ^{1}H-^{13}C COSY (HETCOR) of heated **1**•2H_2O bulk crystals.

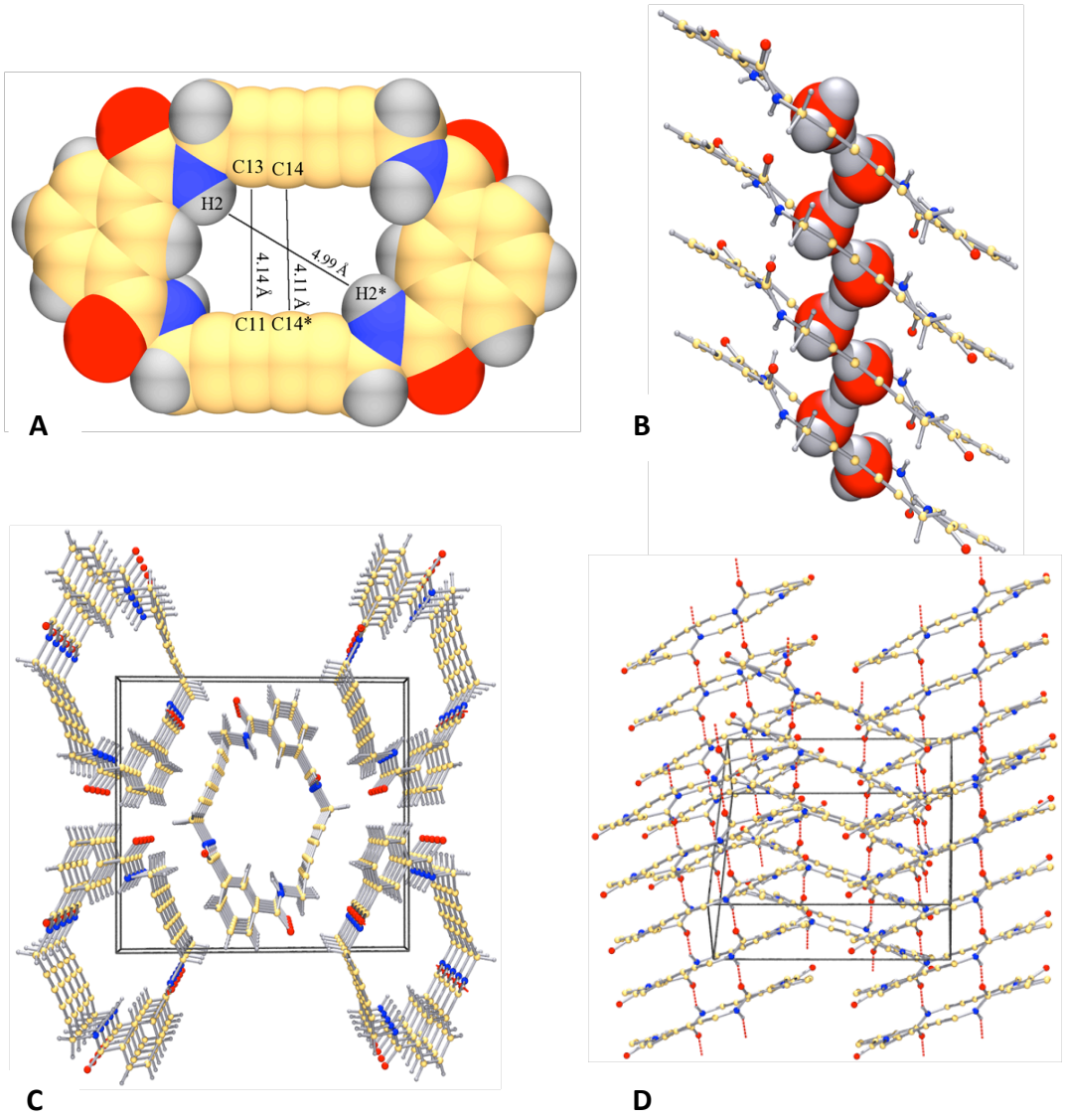

Figure S7. Crystal structure of **1**•2H_2O. (A) Space-filling mode of single macrocycle **1**. (B) Side view of the columnar assembly of **1**, two water molecules were incorporated in each macrocycle. (C) Packing diagram looking down the column axis. (D) Side view of the packing diagram of the crystal.

1•MeOH Crystals

The Raman spectrum (Figure S8) and solid-state UV-vis spectrum of heated **1**•MeOH (Figure S9) indicated the formation of oligodiacetylenes or PDA. Four conformations of the disordered macrocycle for **1**•MeOH crystal are shown in Figure S10.

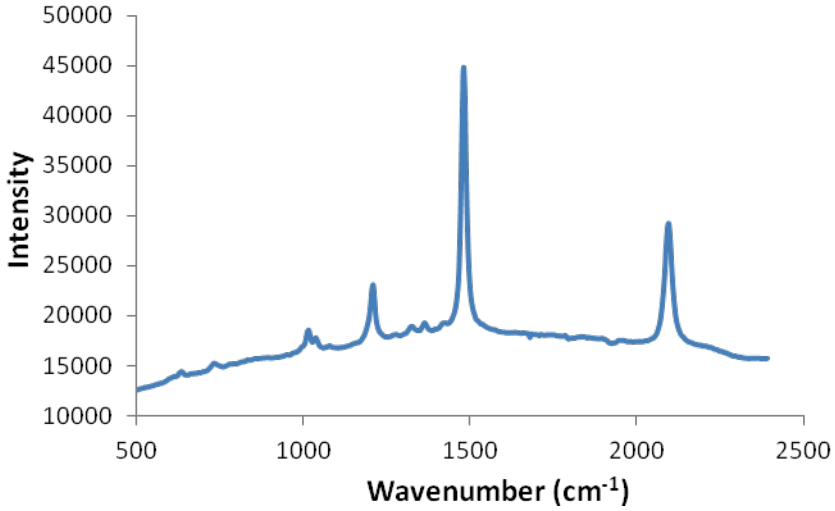

Figure S8. Raman spectrum of heated **1**•MeOH crystal.

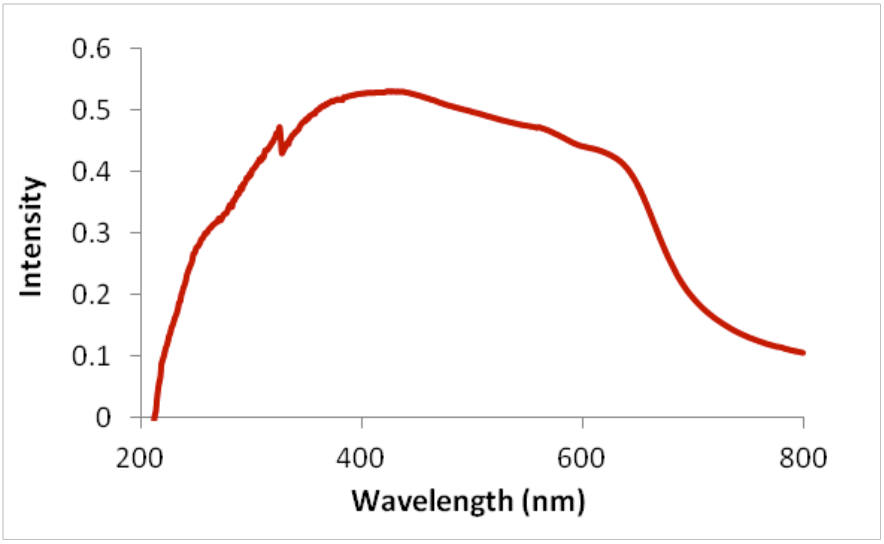

Figure S9. Solid-state UV-vis absorption spectrum of heated **1**•MeOH crystals.

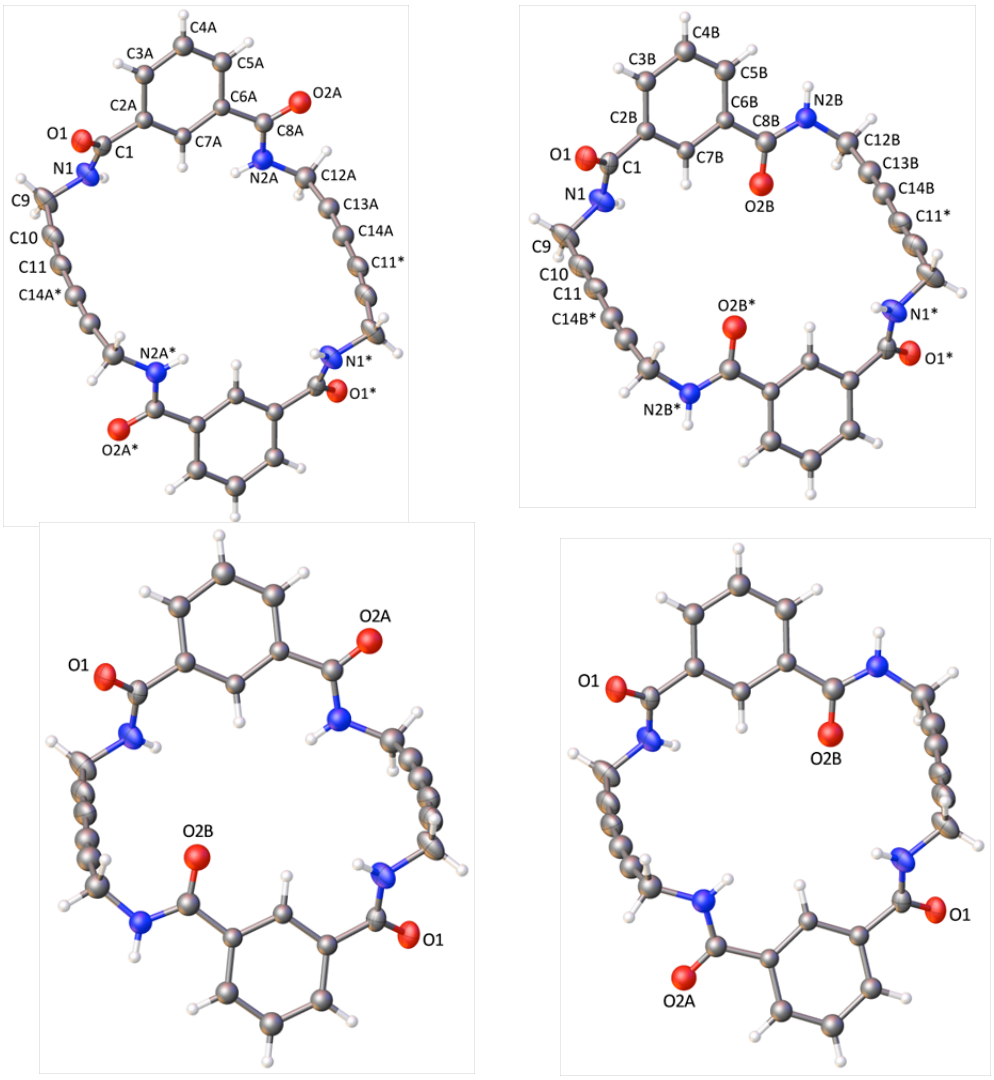

Figure S10. Four different conformations of the disordered macrocycle in **1**•MeOH.

1•4H_2O

Differential scanning calorimetry (Figure S12) was used to investigate the thermal transitions of **1**•4H_2O crystals. These crystals showed two irreversible endothermic transitions at ~100 °C and ~118 °C, respectively, which correspond to the loss of water as observed by TGA (Figure S13). No exothermic transition was observed in the typical range for diacetylene polymerization[2,3], instead, a single exothermic peak was seen at 270 °C. The integration of the peak gave an enthalpy of 275 kJ/mol.

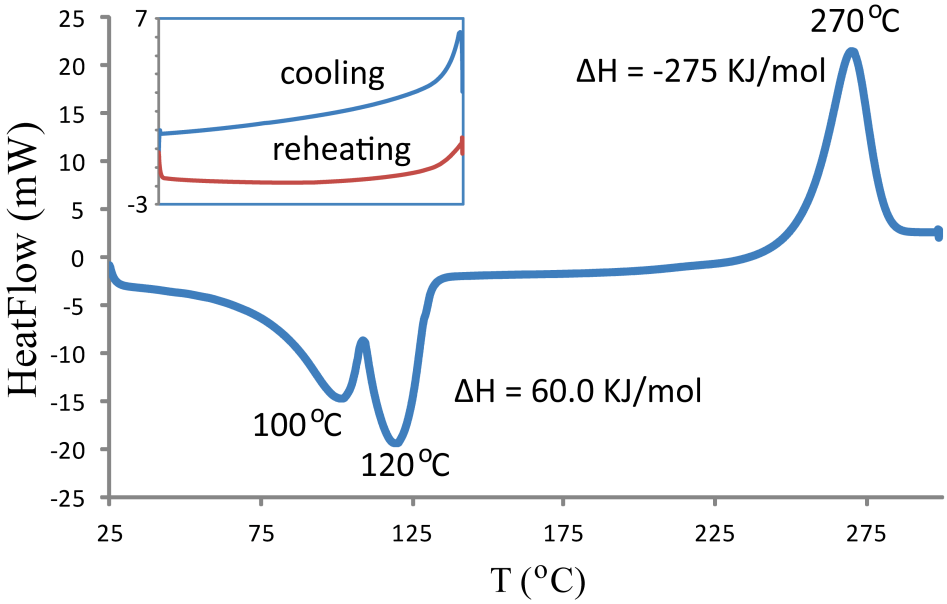

Figure S11. DSC plot of **1**•4H_2O (heating rate 10 °C/min), the inset shows the cooling (10 °C/min) and reheating plot.

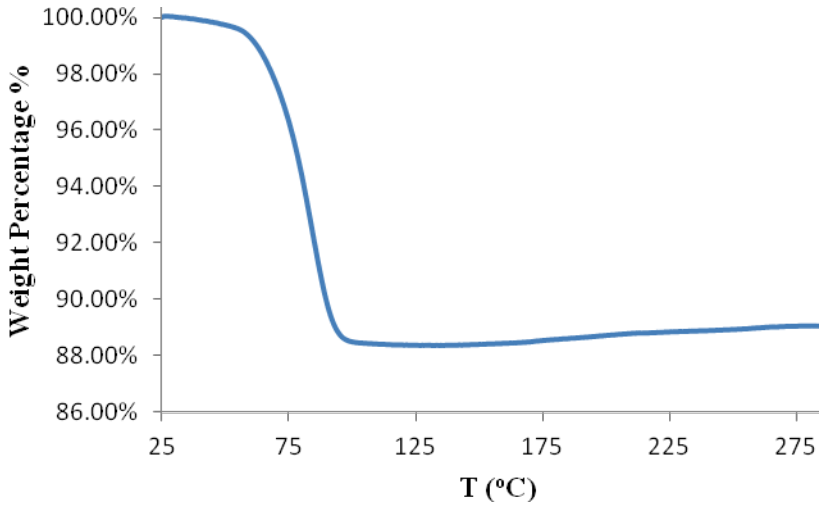

Figure S12. TGA plot of **1**•4H_2O crystals.

According to the crystal structure of **1**•4H_2O, the weight percent of water can be calculated by:

$$Percent\ of\ water = \frac{Molecular\ weight\ of\ water}{Molecular\ weight\ of\ crytstal} = \frac{72}{548.48} = 13.12\%;$$

The weight loss during the heating of the crystals was measured by TGA (Figure S14), a single step desorption with ~ 12% weight loss was observed between 40 °C to 100 °C. Since the weight percent of water in the crystal is around 13%, we can conclude that the weight loss is come from the remove of water.

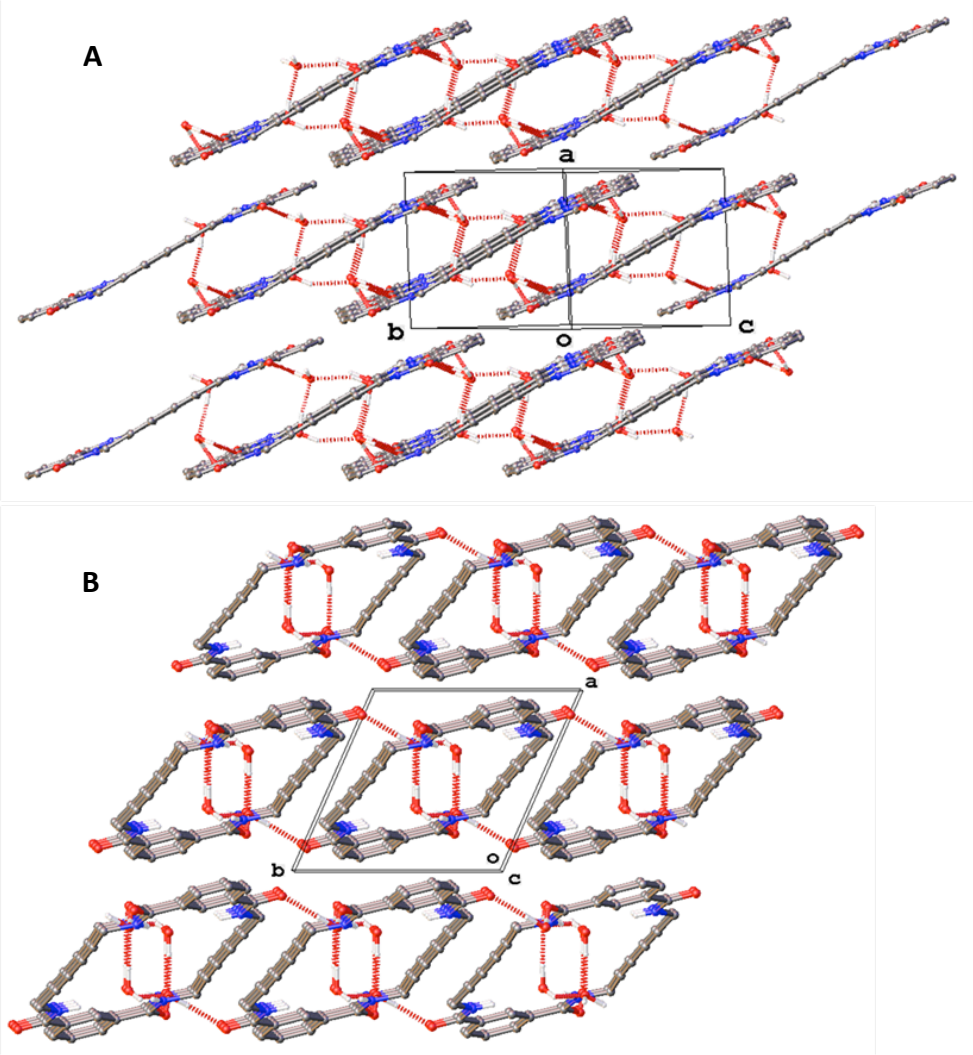

Figure S13. Crystal structure of **1**•4H_2O. (A) View of the hydrogen bonding, 2D sheets made up of tilted macrocycles are formed parallel to the crystallographic (*bc*) plane. (B) Apparent columns were also formed in the crystal. The packing diagram of columns is shown with a view down the *c* axis direction.

Properties of the bulk PDA:

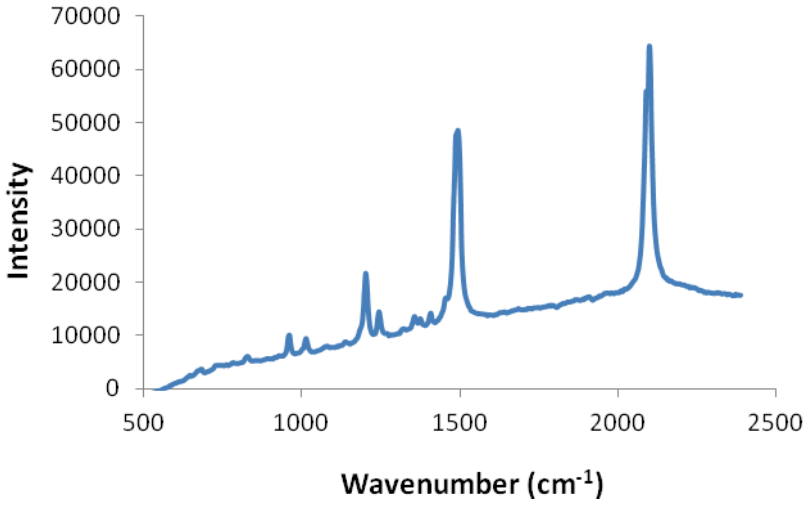

Figure S14. Raman spectrum of bulk PDA formed by the heating of **1**•2H_2O crystals.

Iodine doping of PDA crystals:

Iodine doped PDA crystals (PDA•I_2 complex) were obtained through vapor loading at room temperature. We assembled a special iodine-loading chamber to prevent I_2 surface absorption. The iodine doping system is shown in the schematic below (Figure S16). In this system, flowmeter **1** was used to control the N_2 gas (*F1*), flowmeter **2** was used to control the flow of N_2 gas into the iodine chamber, then iodine vapor was carried out of the chamber by N_2 (*F2*). The two flows mixed together in the loading chamber and the iodine partial pressure PI_2 in the loading chamber was controlled by equation $PI_2 = PI_2^* \times$, where PI_2^* was the vapor pressure of iodine at room temperature. In the iodine doping experiment, we controlled PI_2 to $0.5\ PI_2^*$. Since the partial pressure of iodine in the loading chamber was always lower than the iodine vapor pressure, iodine was unlikely to crystallize on the surface of PDA crystals.

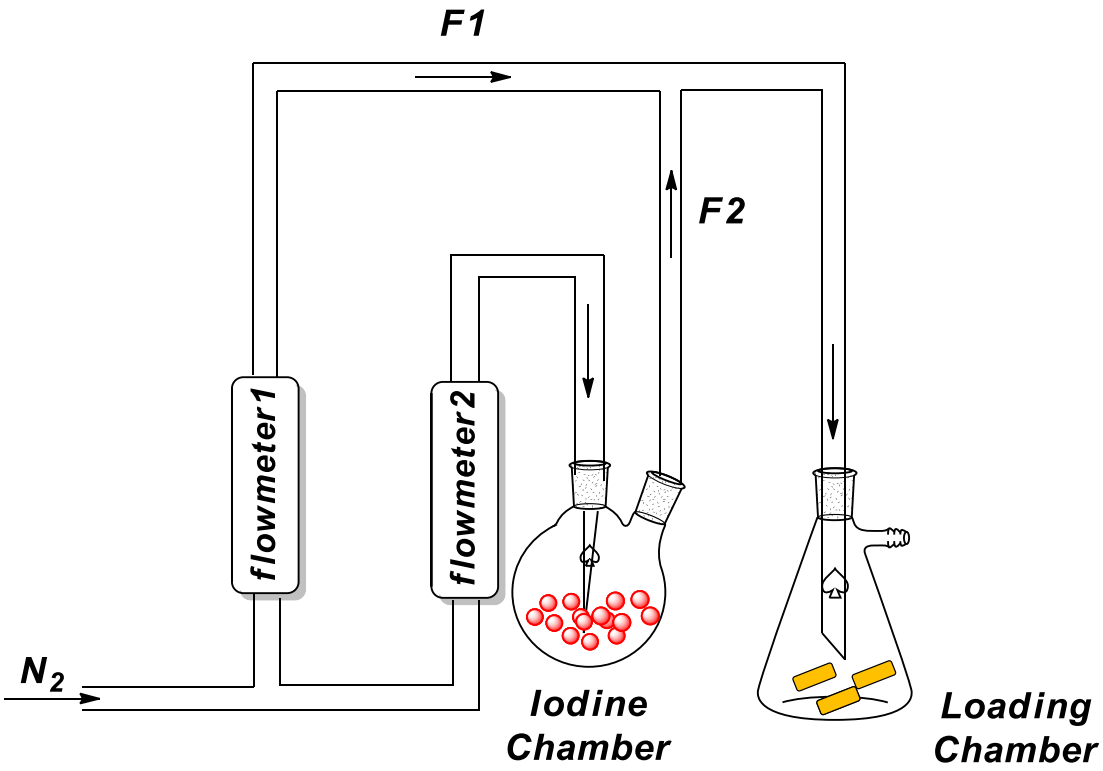

Figure S15. Schematic representation of system designed for iodine doping.

The degree of doping was measured by TGA. Iodine doping reached saturation while keeping PDA crystals in the loading chamber for two days (Figure S17). The iodine to PDA monomer unit ratio was calculated as 1:14 I_2 to PDA.

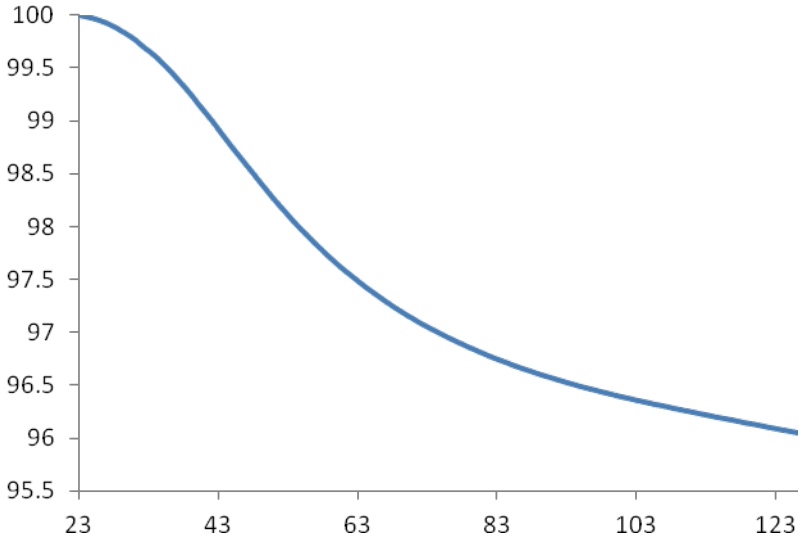

Figure S16. TGA plot of PDA crystal after 48 h iodine doping.

Table S1. Iodine to PDA monomer unit ratio calculated at different doping times.

Doping time (h)	Monomer:I_2
24	21:1
48	14:1
72	13:1
96	14:1

XPS (X-ray photoelectron spectroscopy) was first used to examine the iodine saturated PDA crystals, and the measurements were conducted by using a Kratos AXIS Ultra DLD XPS system, which was equipped with a monochromatic Al Kα source. The monochromatic Al Kα source was operated at 15 keV and 120 W, and the pass energy was fixed at 40 eV for the detailed scans. The binding energy was calibrated using an Ag foil with $Ag3d_{5/2}$ set at 368.21 ± 0.025 eV for the monochromatic Al X-ray source.

Due to the surface charging, a charge neutralizer (CN) was used to do the compensation, and led to the shift of XPS peaks to the lower binding energy area. Therefore the XPS spectra needed to be calibrated before making any comparison. While theoretically there are ten chemically distinct carbon environments in polydiacetylene, in practice XPS may not distinguish between the eight types of hydrocarbons, six from phenyl ring and the rest from the polydiacetylene multiple bonds.[4] Hence, the XPS peaks were corrected according to the core level binding energy (BE) of hydrocarbons which is generally accepted at 284.5 eV.

Table S2. Summarizes the deconvolution results of C 1s, N 1s, O 1s and I $3d_{5/2}$ XPS spectra of empty PDA and PDA•I_2 complex.[5-8]

Table S2. Core Level Binding Energy (BE) Position for PDA crystal before and after Iodine Doping

PDA crystals			I_2 saturated PDA crystals		
Peak	Assignment	BE (eV)	Peak	Assignment	BE (eV)
C 1s	Hydrocarbons	284.5	C 1s	Hydrocarbons	284.5
	CH_2	286.4		CH_2	285.5
	CONH	288.7		CONH	287.6
N 1s	NH	399.9	N 1s	NH	399.4
O 1s	C=O	532.3	O 1s	C=O[1]	532.4
				C=O[2]	531.1
			I $3d_{5/2}$	I_3^-	618.3
				I_5^-	620.4

In order to investigate the interaction of the polyiodide anions with the PDA, we compared the FT-IR (Figure S18) and the solid-state ^{13}C spectra (Figure S19) of PDA and PDA•I_2 complex, but no significant difference was observed. IR spectra of PDA and PDA•I_2 were measured on a Thermo Nicolet Nexus 670 FT-IR spectrometer.

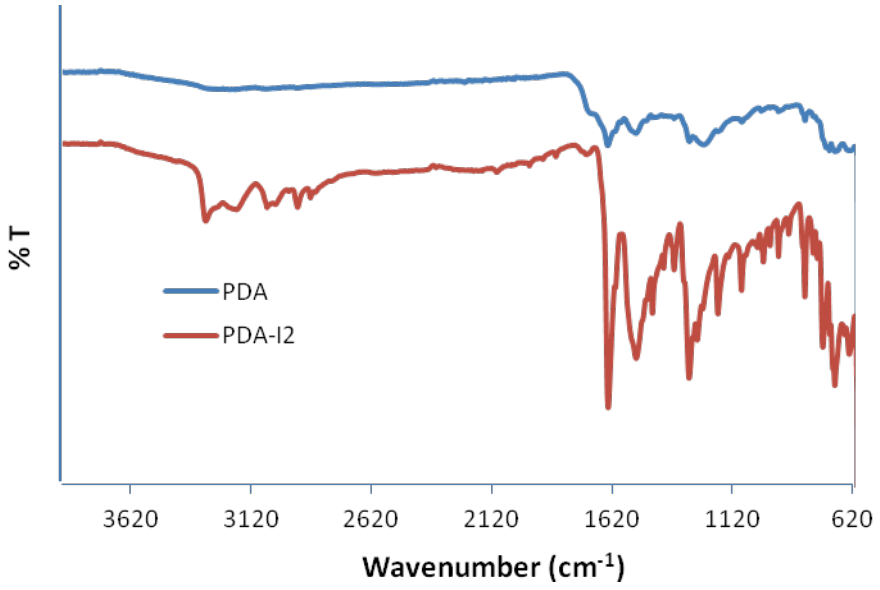

Figure S17. IR spectra of PDA crystals before (blue) and after iodine doping (red).

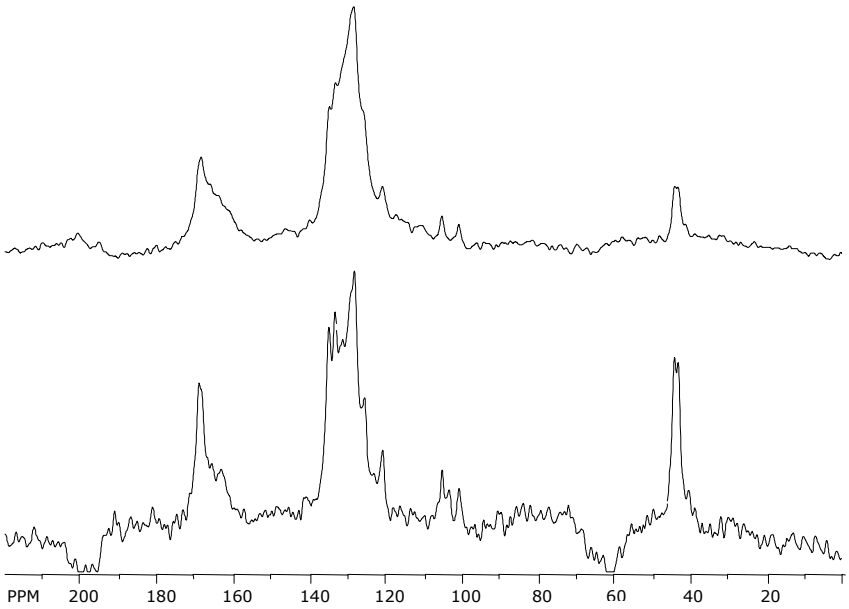

Figure S18. Solid-state ^{13}C NMR of PDA crystals before (bottom) and after iodine doping (top).

PDA microcrystals:

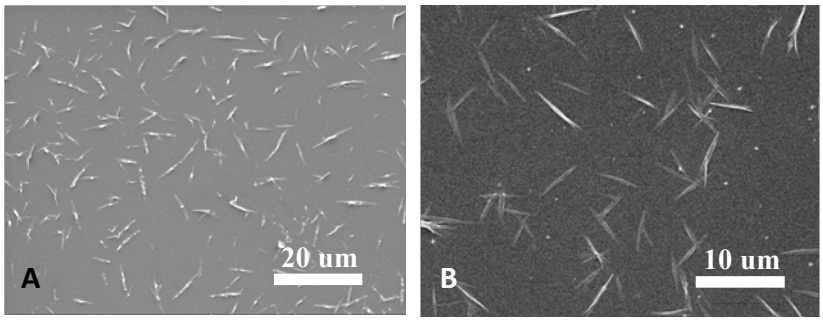

Figure S19. (A) SEM image of polydiacetylene microcrystals generated by spin-coating a 1.0 mg/mL macrocycle **1** solution on a glass slide at a spin-rate of 1000 rpm for 90 s, the spin-coated sample was heated at 190 °C for 3 h to induce the polymerization. (B) PDA microcrystals generated on a quartz slide.

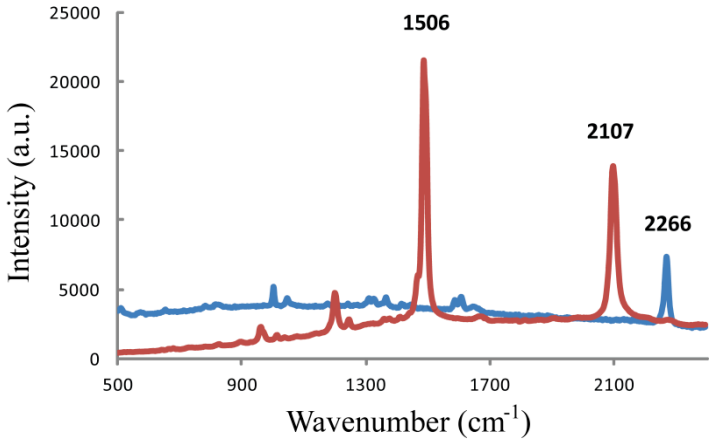

Figure S20. Raman spectra (excitation at 632 nm) of macrocycle **1** microcrystal (blue) and thermal-treated macrocycle **1** microcrystal (red).

TableS3. Peak list of PDA bulk crystal.

2-Theta	d(Å)	Intensity
8.321	10.6175	1123
12.276	7.2042	1086
16.561	5.3487	3105
17.882	4.9564	3029
19.111	4.6402	27
19.312	4.45925	22
21.36	4.1565	291
22.482	3.9515	210
23.314	3.8123	1324
24.068	3.6946	31
24.645	3.6094	463
24.921	3.5701	551
25.56	3.4822	699
26.477	3.3637	331
27.12	3.2854	5
28.838	3.0934	1248
30.561	2.9229	40
32.48	2.7544	121
33.878	2.6438	119

References

(1) Xu, R.; Schweizer, W. B.; Frauenrath, H. *Chem. Eur J* **2009**, *15*, 9105.
(2) Xu, Y. W.; Smith, M. D.; Geer, M. F.; Pellechia, P. J.; Brown, J. C.; Wibowo, A. C.; Shimizu, L. S. *J. Am. Chem. Soc.* **2010**, *132*, 5334.
(3) Zhou, Q.; Carroll, P. J.; Swager, T. M. *J. Org. Chem.* **1994**, *59*, 1294.
(4) Whelan, C. M.; Cecchet, F.; Baxter, R.; Zerbetto, F.; Clarkson, G. J.; Leigh, D. A.; Rudolf, P. *J. Phys. Chem. B* **2002**, *106*, 8739.
(5) Aldissi, M.; Armes, S. P. *Macromolecules* **1992**, *25*, 2963.
(6) Zeng, X. R.; Ko, T. M. *J. Polym. Sci. Part B Pol. Phys.* **1997**, *35*, 1993.
(7) Hsu, S. L.; Signorelli, A. J.; Pez, G. P.; Baughman, R. H. *J. Chem. Phys.* **1978**, *69*, 106.
(8) Grigorian, L.; Williams, K. A.; Fang, S.; Sumanasekera, G. U.; Loper, A. L.; Dickey, E. C.; Pennycook, S. J.; Eklund, P. C. *Phys. Rev. Lett.* **1998**, *80*, 5560.